Chapter 4
Synthesis of Titanium Dioxide: The Influence of Process Parameters on the Structural, Size and Photocatalytic Properties

E.M. Bayan, T.G. Lupeiko, L.E. Pustovaya and A.G. Fedorenko

Abstract The influence of various factors on the photocatalytic activity of titanium dioxide produced from different precursors by a gel and sonochemical methods was analyzed. Obtained nanosized titanium dioxide demonstrates an increased photocatalytic activity, which can be as high as that of the best commercial crystalline powders and even higher. The material with a high photocatalytic activity was prepared from the aqueous solution of titanium chloride by sonochemical method and calcined at 600 °C. The total surface area of the sample is about 50 m^2/g, the phase composition is anatase with a minor proportion of rutile modification.

4.1 Introduction

Due to its low toxicity, chemical stability, low cost, high efficiency in the oxidation of organic and biological objects, nanosized titanium dioxide is the most promising material for photocatalysis, water treatment [1–12]. Parameters affecting the properties of catalysts are porosity, specific surface area, the degree of crystallinity and the ratio of the TiO_2-crystalline modifications (anatase, rutile, brookite). Among these modifications of titanium dioxide anatase is considered to be the most effective photocatalytic phase [13, 14]. However, as it is stated in the work of Zŭnic et al. [15], a small addition of rutile to anatase increases the photocatalytic activity of the material due to the synergistic effect between rutile and anatase, which increases the lifetime of the charge carriers. Titanium dioxide in various phase compositions can be produced by choosing the method of synthesis or through varying its parameters (precursor concentration, temperature, duration of process,

E.M. Bayan (✉) · T.G. Lupeiko · A.G. Fedorenko
Faculty of Chemistry, Southern Federal University, Rostov-on-Don, Russia
e-mail: ekbayan@sfedu.ru

L.E. Pustovaya
Don State Technical University, Rostov-on-Don, Russia

I.A. Parinov et al. (eds.), *Advanced Materials*, Springer Proceedings in Physics 175, DOI 10.1007/978-3-319-26324-3_4

etc.) [16, 17]. Practical application of photocatalytic reactions requires the maintenance of light intensity in order to achieve sufficient energy rates that exceeds TiO_2 band gap energy (BGE). Anatase and brookite are known to have BGE = 3.2 eV, BGE (rutile) = 3.02 eV, the absorption thresholds corresponding to 380 and 410 nm, respectively [18]. Various methods to prepare TiO_2-based photocatalysts are available including combustion titanium chloride in oxygen stream, vapor-phase or hydrothermal hydrolysis and others [19–22]. In recent years, sol-gel method, which allows one to obtain nanoparticles with desired properties has attracted close attention [23–28]. Sonochemical method is a relatively new method to prepare nanocrystalline materials [15, 29]. Compared with conventional synthetic methods, sonochemical synthesis yields materials with a high specific surface area and a better thermal stability [15].

The main objective of this study was to prepare nanosized titanium dioxide characterized by higher photocatalytic properties compared with existing analogues obtained via gel technology and sonochemistry from different precursors such as titanium chloride and titanyl nitrate. Different physical properties and photocatalytic activity of the synthesized materials were compared.

4.2 Experimental Methods

4.2.1 Materials

All reagents used were commercially obtained and used without any further purification. All solutions were prepared using deionized water.

4.2.2 Photocatalyst Preparation

TiO_2 nanocrystallites were synthesized from aqueous solutions of titanium chloride (pure $TiCl_4$ liquid was carefully diluted with ice water to a transparent colorless aqueous solution) or titanyl nitrate, $TiO(NO_3)_2$ with concentration $[Ti^{4+}] = 0.1$ M. Ammonia solution (10 %) was added to these solutions drop wise until white precipitates (gel) were obtained and the pH = 8. The temperature of aqueous solutions varied from 0 to 100 °C. Some precipitates were obtained in the Ultrasonic Cleaning Units (Elma D-78224) under sonication (Ultrasonic power effective 280 W, frequency 50–60 Hz). The precipitates were washed with deionized water until chlorine or nitrate ions became undetectable. Then the gels were dried and calcined at the different temperature selected according DTA/TG-analysis (450, 600, 700 °C) for 30, 60, 120 min. Synthesis parameters are summarized in Table 4.1. Degussa P25 (P25) was applied as a reference for comparison.

Table 4.1 Conditions for the synthesis; characteristics of synthesized samples

Series of samples	Precursor	Synthesis temperature (°C)	Sonication	Calcined temperature (°C)	Sample after calcination	Crystallite size (nm)	Structure[a]
1	$TiCl_4$	≤5	−	700	1.1	18	A
				600	1.2	13	A
				450	1.3	9	A
2	$TiCl_4$	80	+	700	2.1	22	A + R
				600	2.2	18	A + R
				450	2.3	9	A + R
3	$TiCl_4$	≤20	+	700	3.1	20	A
				600	3.2	14	A
				450	3.3	9	A
4	$TiO(NO_3)_2$	≤5	−	700	4.1	23	A
				600	4.2	12	A
				450	4.3	8	A
5	$TiO(NO_3)_2$	80	+	700	5.1	11	A
				600	5.2	9	A
				450	5.3	6	A

[a] *A* anatase, *R* rutile

4.2.3 Materials Characterization

X-ray powder diffraction (XRD) analysis was carried out using an ARL X'TRA diffractometer equipped with a high-intensity Kα1 irradiation (λ = 1.540562 Å) operated at 40 kV and 30 mA. Typical scans were performed in a wide range of Bragg angle ($20° \leq 2\theta \leq 60°$). The XRD patterns were analyzed using the standard JCPDS files. Qualitative analysis of phase state was performed by using data PDF-2 data base and PCPDFWIN software.

The average particle size and total surface area of the samples were determined by sedimentation analysis in a CPS Disk Centrifuge Model DC24000.

Coherent scattering region was calculated from the X-ray line broadening, according to the Debye-Scherrer equation:

$$d = \lambda/(\beta \cos\theta), \tag{4.1}$$

where λ = 0.1540562 nm is the X-ray wave length, β is the full width at half maximum (FWHM) of the diffraction peak (101) for anatase and (110) for rutile, θ is the diffraction angle.

Thermogravimetry (TGA) and Differential Thermal Analysis (DTA) of the samples were carried out using a thermal analyzer (STA 449°S/4 G Jupiter Jupted) at a heating rate of 10 °C/min from 283 to 1000 K.

The morphological characteristics were analyzed with transmission electron microscopy utilizing a TEM Tecnai G^2 Spirit Bio TWIN operating at 120 kV.

4.2.4 Photocatalytic Activity Measurements

The photocatalytic activity of the prepared samples in the aqueous media was evaluated through monitoring of the discoloration of organic azo dye methylene blue (MB, $C_{16}H_{18}N_3SCl$) or methyl orange (MO, $C_{14}H_{14}N_3O_3SNa$). In a typical measurement, TiO_2 power (1 g/l) was suspended in MB (or MO) aqueous solution (20 mg/l) by stirring. Experiments were carried out at room temperature in quartz glass beakers. 125 W medium pressure mercury lamp was used as the UV light source. Residual concentration of the MB solutions was analyzed by mass spectrometry (Spectrophotometer UNICO 1201). Recycling test was subsequently performed three times.

4.3 Results and Discussion

4.3.1 DTA/TGA Measurements

Figure 4.1 demonstrates the removal of a large part of sample mass at temperatures up to 180 °C due to the release of water. The exothermic peak in the DTA pattern at 437 °C corresponds to degradation of titanium hydroxide along with formation of anatase crystalline phase. The exothermic peak at 500–700 °C at a constant mass of the sample is apparently associated with a new phase transition (presumably anatase-rutile). As a result, calcination temperatures of the samples were selected: 450, 600 and 700 °C.

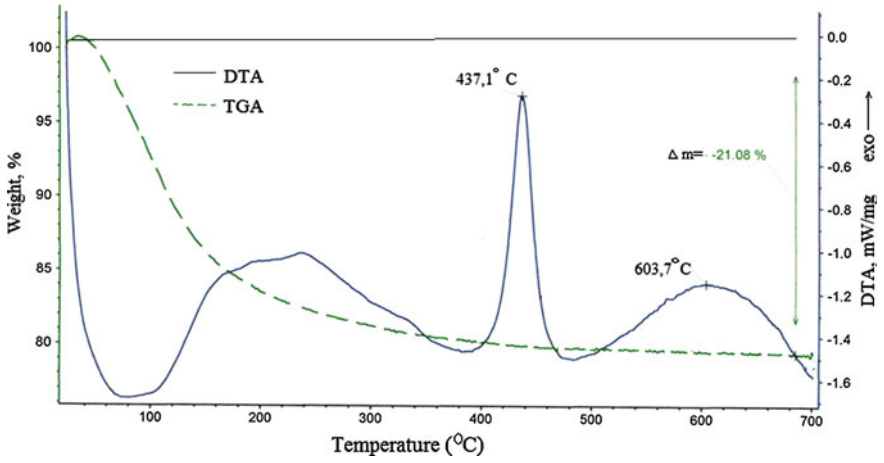

Fig. 4.1 DTA/TGA patterns of the sample prepared

4.3.2 Structural and Size Characterizations

According to XRD, the samples were found to preserve their amorphous structure after calcination for 30 min, after 60 min calcination the mixture of amorphous and crystallized phase was detected, after 120 min calcination the anatase phase was stated to be prevailing. Based on these data, the calcination was carried out for 120 min in further experiments. Longer calcination of the samples resulted in the formation of rutile phase and the increase of crystallite size.

XRD patterns demonstrated that all samples of 1, 3–5 series (Table 4.1) had anatase modification; the degree of their crystallinity grew with increasing temperature. Samples of series 2 (Fig. 4.2) had a mixture of anatase and rutile, the proportion of rutile in the mixture increased with increasing temperature. XRD data (Fig. 4.3) for samples synthesized from titanyl nitrate suggest stabilization of anatase modification under above-mentioned conditions of synthesis.

In assessing the coherent scattering regions by Scherrer method, it was found that the average crystallites size increases with grooving calcination temperature and equals 6–9 nm (450 °C), ~15 nm (600 °C), ~20 nm (700 °C). It could be explained by the processes of titanium dioxide crystallization.

TiO_2 synthesized via the gel-precipitation from titanium chloride consisted of particles with anatase sizes of 9–18 nm depending on the calcination temperature. The size of detected particles for the gel-precipitation samples obtained from titanyl nitrate solutions equals 8–23 nm. The smallest TiO_2 particles of 6–11 nm were prepared by sonochemical method from titanyl nitrate solutions.

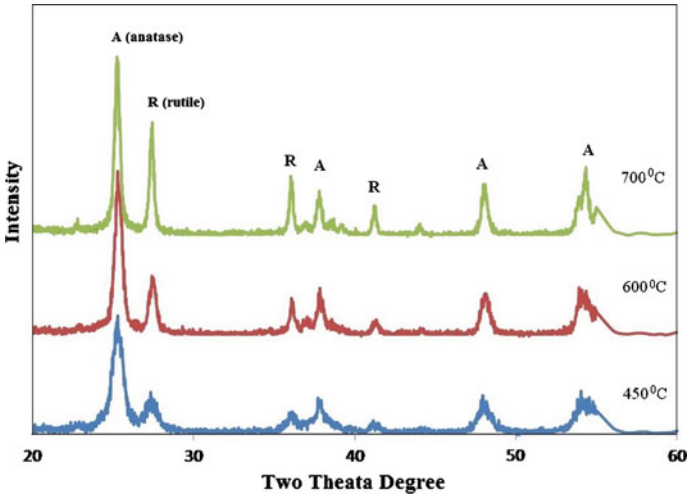

Fig. 4.2 XRD patterns of the samples prepared from titanium chloride and calcined at different temperatures

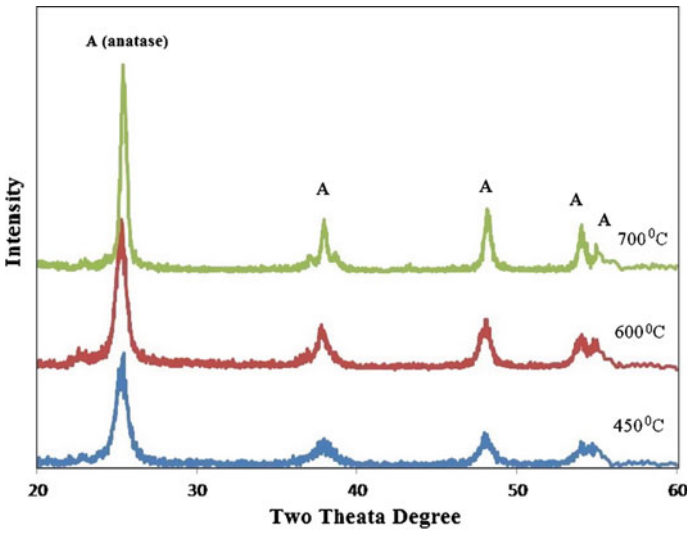

Fig. 4.3 XRD patterns of the samples prepared from titanyl nitrate and calcined at different temperatures

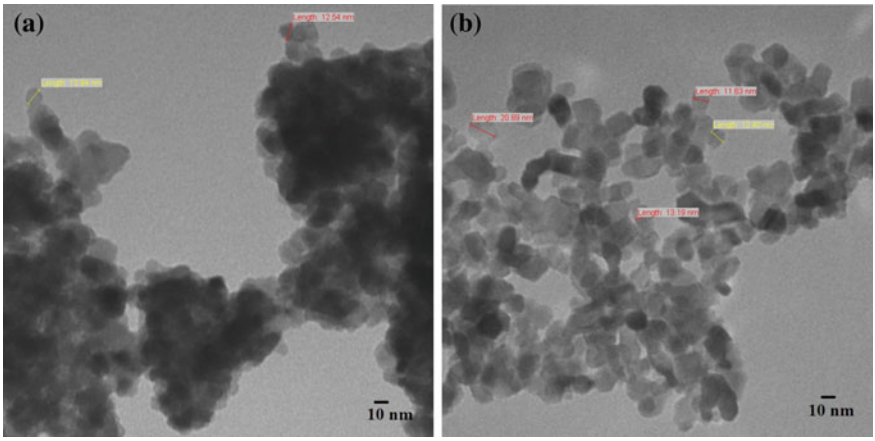

Fig. 4.4 TEM microphotographs of TiO_2 powders: the sample 1.1 (**a**), the sample 2.2 (**b**)

Figure 4.4 presents the TEM microphotographs of TiO_2 powders. The microphotographs emphasize that sizes of titanium dioxide grains increase with the sonochemical treatment.

Sedimentation analysis revealed that the total surface area of prepared samples was about 50 m^2/g.

4.3.3 Photocatalytic Performance

Photocatalytic activities of TiO_2 were evaluated by the degradation of MB and MO.

Figures 4.5 and 4.6 demonstrate that the samples prepared by sonochemical method are characterized by far better photocatalytic activities. However, the effect of calcination temperature is different for different sample series. The highest photocatalytic activity by MB from the 1 and 3 series is shown by samples 1.1 and 3.1, respectively, calcined at 700 °C. However, the highest photocatalytic activity from the 2-nd series is demonstrated by sample 2.2, which was calcined at 600 °C. It could be explained by the fact that sample 2.1, which was calcined at 700 °C contains considerable amount of rutile, which did not have photocatalytic activity.

Figure 4.7 demonstrates low photocatalytic activities for 1 and 2 series samples with respect to methyl orange which was the same or lower than that of Degussa P25. It should be noted that observed photocatalytic activity is lower with respect to the MO than that with respect to the MB for all series of samples (Figs. 4.5, 4.6 and 4.7).

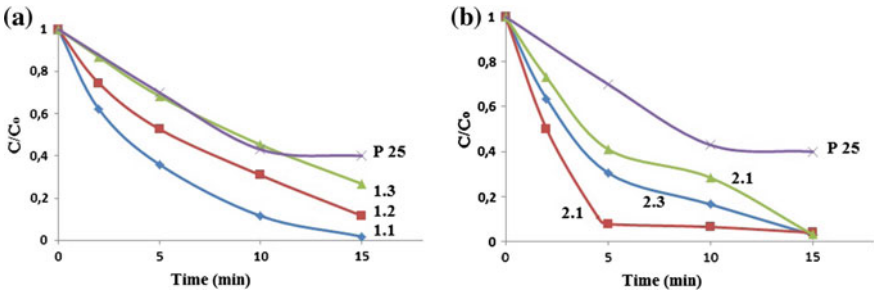

Fig. 4.5 Degradation profiles for TiO_2 samples of the 1 series (**a**) and the 2 series (**b**) with respect to methylene blue

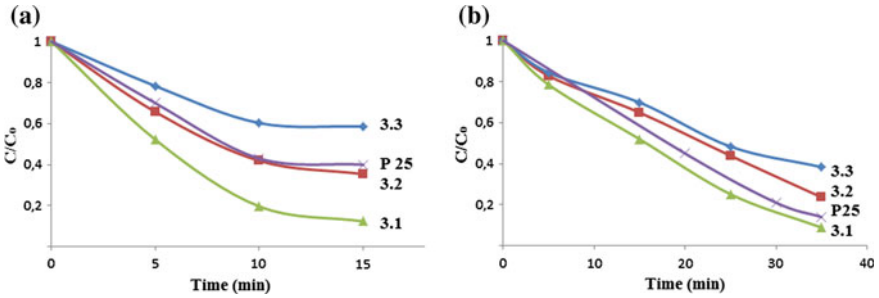

Fig. 4.6 Degradation profiles for TiO_2 samples of 3 series with respect to methylene blue (**a**) and methyl orange (**b**)

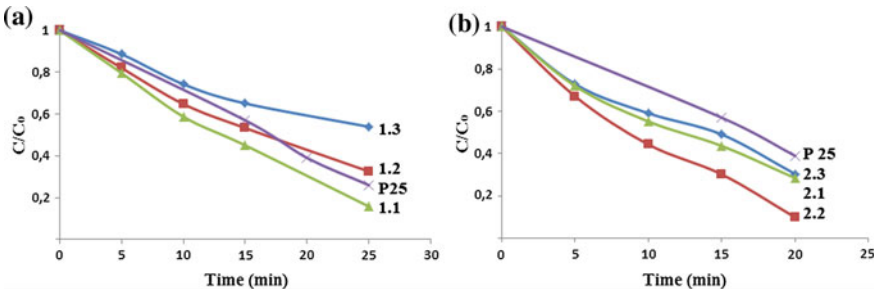

Fig. 4.7 Degradation profiles for TiO_2 samples of the 1 series (**a**) and the 2 series (**b**) with respect to methyl orange

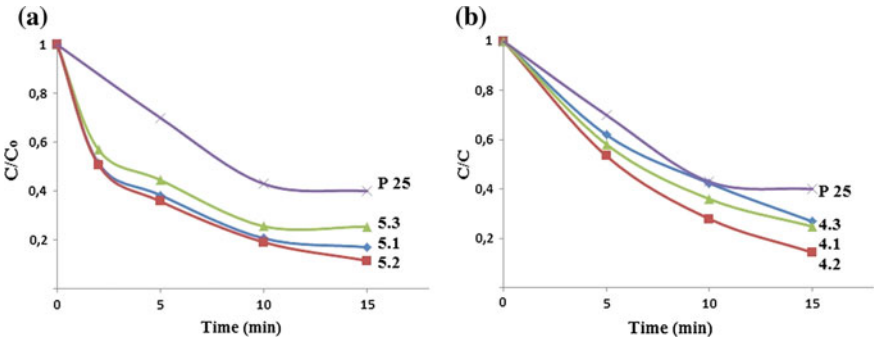

Fig. 4.8 Degradation profiles for TiO_2 samples of the 5 series (**a**) and the 4 series (**b**) with respect to methylene blue

Photocatalytic activities for 4 and 5 series samples obtained from titanyl nitrate are lower than that for 1, 2 and 3 series samples which were synthesized from titanium chloride (Fig. 4.8).

4.4 Conclusions

We have found that the precursors (aqueous solutions of titanium chloride and titanyl nitrate) do not demonstrate essential influence on the final value of photocatalytic activity but determine significantly the time of photodegradation process.

Thus, the samples synthesized from aqueous solution of titanium tetrachloride demonstrate higher rate of photodegradation process than the ones synthesized from nitrate solutions. It has been established that sonochemical method enables us to obtain samples with the best photocatalytic properties (the best sample is 2.2). High photocatalytic activity of the sample 2.2 can be explained by its structure (Fig. 4.2). When comparing XRD patterns for 2nd series samples, it was determined that these

samples had small proportion of rutile modification and significant amounts of anatase. This is probably due to the use of $TiCl_4$ as a precursor in combination of high temperature (80 °C) at the synthesis stage and ultrasonic treatment, which leaded to the formation of nanocrystalline anatase phase domains with inclusions of rutile phases and heterophase particles formation. The optimal values of quantum yield are known to be obtained on heterophase particles, because photogenerated charge of heterophase are particles spatially separated, recombination is also hindered [15]. So, photocatalytic activity of nanosized titanium dioxide obtained this way is higher than that of Degussa P25. The synthesis of produced titanium dioxide was performed from the aqueous solutions of titanium chloride at 80 °C by sonochemical method with calcination at 600 °C. The best sample was obtained with a total surface area of about 50 m^2/g, the size was estimated to be 20 nm, its phase composition being anatase with a minor proportion of rutile. It is determined that the methods which enable us to obtain a biphasic system (anatase and rutile) are promising for further synthesis of materials with high photocatalytic activity.

Acknowledgments This research was supported by the Project Part of the State Assignment for Research (Ref. No. 4.2592.2014/K).

References

1. F. Han, V.S.R. Kambala, M. Srinivasan, D. Rajarathnam, R. Naidu, Appl. Catal. A **359**, 25 (2009)
2. H. Xu, S. Ouyang, L. Liu, P. Reunchan, N. Umezawa, J. Ye, J. Mater. Chem. B. **32**, 12642 (2014)
3. Y. Xie, O. Zhao, X.J. Zhao, Y. Li, Catal. Lett. **118**, 231 (2007)
4. H.U. Lee, G. Lee, J.C. Park, Y.-C. Lee, S.M. Lee, B. Son, S.Y. Park, C. Kim, S. Lee, S.C. Lee, Chem. Eng. J. **240**, 91 (2014)
5. H. Khan, Dimitrios Berk, Catal. Lett. **144**, 890 (2014)
6. J. Choi, H. Lee, Y. Choi, S. Kim, S. Lee, S. Lee, W. Choi, J. Lee, Appl. Catal. B: Environ. **147**, 8 (2014)
7. A.R. Khataee, M.B. Kasiri, J. Mol. Catal. A: Chem. **328**, 8 (2010)
8. A. Di Paola, E. García-López, G. Marcì, L. Palmisano, J. Hazard. Mater. **211–212**, 3 (2012)
9. M.N. Chong, B. Jin, C.W.K. Chow, C. Saint, Water Res. **44**, 2997 (2010)
10. U.I. Gaya, A.H. Abdullah, J. Photochem. Photobiol., C **9**, 1 (2008)
11. K. Hashimoto, H. Irie, A. Fujishima, Jpn. J. Appl. Phys. Part 1: Regul. Pap. Short Notes Rev. Pap. **44**, 8269 (2005)
12. M. Răileanu, M. Crişan, I. Niţoi, A. Ianculescu, P. Oancea, D. Crişan, L. Todan, Water. Air Soil Pollut **224**, 1548 (2013)
13. D.C. Hurum, A.G. Agrios, K.A. Gray, T. Rajh, M.C. Thurnauer, J. Phys. Chem. B **107**, 4545 (2003)
14. C. Wu, Y. Yue, X. Deng, W. Hua, Z. Gao, Catal. Today **93–95**, 863 (2004)
15. V. Zŭnic, M. Vukomanović, S.D. Škapin, D. Suvorov, J. Kovac, Ultrason. Sonochem. **21**, 367 (2014)
16. M. Dawsot, G.B. Soares, C. Ribeiro, J. Solid State Chem. **215**, 211 (2014)
17. Z. Ismagilov, L.T. Tsikoza, N.V. Shikina, V.F. Zarytova, V.V. Zinovev, S.N. Zagrebelny, Usp. **78**, 942 (2009)

18. M. Pelaeza, N.T. Nolanb, S.C. Pillaib, M.K. Seeryc, P. Falarasd, A.G. Kontosd, P.S.M. Dunlope, J.W.J. Hamiltone, J.A. Byrnee, K. O'Sheaf, M.H. Entezarig, D.D. Dionysiou, Appl. Catal. B **125**, 331 (2012)
19. J.Q. Qi, Y. Wang, W.P. Chen, H.Y. Tian, L.T. Li, H.L.W. Chan, J Alloy Compd **413**, 307 (2006)
20. T.K. Tseng, Y.S. Lin, Y.J. Chen, H. Chu, Int. J. Mol. Sci. **11**, 2336 (2010)
21. J. Lin, Y. Lin, P. Liu, J.M. Meziani, L.F. Allard, Y.P. Sun, J. Am. Chem. Soc. **124**, 11514 (2002)
22. F.A. Deorsola, D. Vallauri, Powder Technol. **190**, 304 (2009)
23. U.G. Akpan, B.H. Hameed, Appl. Catal. A **375**, 1 (2010)
24. M. Răileanu, M. Crişan, N. Drăgan, D. Crişan, A. Galtayries, A. Brăileanu, A. Ianculescu, V. S. Teodorescu, I. Niţoi, M. Anastasescu, J. Sol-Gel. Sci. Technol. **51**, 315 (2009)
25. T.K. Tseng, Y.S. Lin, Y.J. Chen, H. Chu, Int. J. Mol. Sci. **11**, 2336 (2010)
26. W.H. Ching, M. Leung, D.Y.C. Leung, Sol. Energy **77**, 129 (2004)
27. N. Arconada, A. Durán, S. Suárez, R. Portela, J.M. Coronado, B. Sánchez, Y. Castro, Appl. Catal. B **86**, 1 (2009)
28. J.H. Schattka, D.G. Schukin, J. Jia, M. Antonietti, R.A. Caruso, Chem. Mater. **14**, 5103 (2002)
29. B. Neppolian, Q. Wang, H. Jung, H. Choi, Ultrason. Sonochem. **15**, 649 (2008)